AIAA-2000-4423

THE IMPACT OF ALTIMETER RANGE OBSERVATIONS ON NEAR NAVIGATION

J.J. Bordi, J.K. Miller, and B.G. Williams
Jet Propulsion Laboratory, California Institute of Technology,
Pasadena, California

R.S. Nerem and F.J. Pelletier
Center for Space Research, The University of Texas at Austin
Austin, Texas

Abstract

The Near Earth Asteroid Rendezvous (NEAR) spacecraft is currently in the early part of the orbit phase around the asteroid Eros. Altimeter range measurements from the LIDAR instrument aboard NEAR are processed in combination with the primary tracking data types, including Deep Space Network (DSN) tracking and optical landmark tracking. As a backup observation type, the LIDAR measurements are not used to generate the operational orbits. Analysis of the impact of the altimeter observations on the estimation of the Eros shape model and the NEAR orbits is performed. The analysis includes an assessment of the impact of altimeter observations on solution convergence when different a priori shape models are used and when different combinations of tracking data are used. The effectiveness of using the LIDAR observations to estimate the shape model while holding the orbits fixed is examined, and similarly the effect of estimating the orbits while holding the shape model fixed is examined.

Introduction

The Near Earth Asteroid Rendezvous (NEAR) spacecraft was inserted into orbit around the asteroid Eros on February 14, 2000. A complete overview of the NEAR spacecraft and mission design is provided in Farquhar[1] and Farquhar et al.[2] As the first spacecraft to orbit a small body, it has provided many unique challenges and opportunities in the area of spacecraft navigation. One area of investigation is assessing the value of using altimeter range measurements as an observation type in spacecraft navigation. The Laser Altimeter Range (LIDAR) instrument onboard NEAR supplies the altimeter range measurements. However, the LIDAR observations are not used as one of the primary tracking types in producing the operational NEAR ephemerides. The primary tracking types include Deep Space Network (DSN) radiometric Doppler and range observations as well as optical landmark tracking. The purpose of this study is to see if the addition of altimeter range data in the orbit determination procedure can improve not only the orbits, but also the estimates of the central body's physical parameters.

The altimeter provides a measure of the distance from the spacecraft to the point on the surface of the body being illuminated. An advantage of the altimeter data is that the measurements can be taken continuously, without the sunlight restrictions of optical landmark tracking, or the station visibility restrictions of DSN tracking. On the other hand, the altimeter range measurements are weakened by the fact that they are made relative to the surface, which is an unknown height above the body's center of mass. Therefore, the shape model usually needs to be estimated simultaneously with the spacecraft's orbit, in order to prevent errors in the surface model from being aliased into the orbits. The temporal and geographical density of the observations make it feasible to estimate both the shape model and the orbit at the same time, provided that there is a sufficient amount of a complimentary data type available (e.g., DSN radiometric or optical tracking).

The asteroid Eros is shaped irregularly, with the principal semi-axes measuring 16.5, 8.0, and 6.5 km. For a description of Eros, see the paper by Miller[3] which provides the current best estimates of the Eros physical parameters. After orbit insertion, NEAR orbited Eros at relatively high altitudes, ranging from 500 to 200 km. This made the initial orbit phase not very useful for assessing the performance of the LIDAR instrument on spacecraft navigation, since the instrument was designed to be most effective at a range of 50 km. Additionally, during this timeframe NEAR was orbiting Eros at fairly low inclinations. This meant that large areas of the asteroid were not covered by altimeter observations. This is important, since in order to get a good estimated of the Eros shape model a good geographical distribution of altimeter measurements is needed. For these reasons, this study concentrates on the orbit phase beginning on April 2, 2000. This date coincides with the maneuver that put NEAR in a 200 x 100 km transfer orbit with an inclination of 57 degrees. On April 11, NEAR was inserted into a near circular 100 km orbit with an inclination of 59 degrees. Then, on April 22, NEAR was placed in 100 x 50 km transfer orbit, with an inclination of 64 degrees. This orbit was maintained until April 30, when the spacecraft was inserted into a near circular 50 km polar orbit. Obviously, the circular 50 km polar orbit would provide the best opportunity for assessing the impact of the LIDAR observations, since the altitude is equal to what the instrument was designed to operate at and the polar orbit will provide global coverage of Eros. However, due to time constraints on the publication of this paper, only a small portion of the 50 km orbit phase is analyzed in this study. For more detailed information on the NEAR orbital plan see the paper by Helfrich et al.[4]

Table 1

A PRIORI UNCERTAINTIES FOR ESTIMATED PARAMETERS

Parameter		Uncertainty
Spacecraft position		100 km
Spacecraft velocity		20 mm/s
Asteroid position		60 km
Asteroid velocity		20 mm/s
Asteroid orientation –	prime meridian	10 deg
	Spin axis angles	1 deg
Asteroid orientation rate		0.02 deg/s
Stochastic Accelerations (1 hour)		0.5 nm/s^2
Solar Pressure:		
Gamma		0.01
Beta		0.01
Effective thermal emissivity of spacecraft		0.1%
Maneuver Errors		5 mm/s
Landmark Locations		700 m
Normalized Gravity Harmonics (8x8)		0.1 - 0.04

The Reference Orbits

The NEAR operational orbits are used as reference orbits in this study. These orbits are computed using both the DSN and optical landmark tracking data. These reference orbits are used for comparison purposes, in an effort to provide a benchmark for the orbits computed using the LIDAR data. When the reference orbits are computed, the parameters outlined in Table 1 are estimated. This table also includes the a priori uncertainties assigned to each of these parameters.

The reference orbits are computed with the observation data weighted as follows: the Doppler data is assigned an uncertainty of 0.0056 Hz, the radiometric range observations are weighted with an uncertainty of 700 km, and the optical landmark tracking is processed with an a priori uncertainty of 1 pixel. For a data arc spanning April 2 through May 4, the RMS of the 22,777 Doppler residuals is 0.0021 Hz, the RMS of the 6270 radiometric range residuals is 120 km, and the RMS of the 6,270 optical residuals is 1.04 pixels. The reference orbits are assumed to be accurate to about the 50 meter level. This assumption is based on the data residuals, a posteriori formal uncertainties, consistency of the solutions, and analysis of the estimated physical parameters.

Processing the Altimeter Observations

The orbit determination software used in this study (Jim Miller's PCODP3) is the operational navigation software used for the NEAR mission and has been written to process DSN radiometric, optical, and altimeter measurements. The formulation used to process the altimeter range measurements is outlined in the paper by Bordi et al.[5] To try to account for systematic errors in the altimeter range observations, several kinematic parameters can be estimated. These parameters include a standard range bias. Additionally, a factor is estimated that is intended to account for any performance degradation that may occur in the LIDAR instrument as the range from the instrument to the illuminated surface point increases. This parameter is based on the fact that the LIDAR signal weakens an amount proportional to the square of the range. This results in the two-way signal being weakened by an amount proportional to the range to the forth power. These parameters are then added to the computed observation as follows:

$$\begin{aligned} Y_{Alt} = & \left\| \vec{R}_{s/c} - \vec{R}_{Sur} \right\| + R_{Bias} + \\ & F_{Degr} \cdot \left(\left\| \vec{R}_{s/c} - \vec{R}_{Sur} \right\| \right)^4 + \varepsilon \end{aligned} \tag{1}$$

In the equation, $\vec{R}_{s/c}$ is the position of the spacecraft relative to the center of mass, $\vec{R}_{Sur}$ is the position of the point on the surface of the central body that is illuminated by the altimeter, and ε is the error in the observation. The estimated parameters are the range bias, R_{Bias}, and the degradation factor, F_{Degr}.

A pointing offset can also be estimated. This parameter is intended to account for a slight misalignment of the LIDAR instrument that would result in a pointing error with respect to the predefined spacecraft-fixed instrument pointing direction. One cause for such a misalignment could be heat buildup in the spacecraft bus, resulting in flexure of the panels that the LIDAR instrument is mounted to. The partial of these pointing offsets with respect to the spacecraft position is calculated as follows:

$$\begin{aligned} \frac{\partial R_{Alt}}{\partial Att_x} &= \left(T_{inert}^{s/c} \frac{\partial R_{Alt}}{\partial \vec{R}_{s/c}} \right)_{x s/c} \cdot \frac{\partial x_{s/c}}{\partial Att_x} \\ &= \left(T_{inert}^{s/c} \frac{\partial R_{Alt}}{\partial \vec{R}_{s/c}} \right)_{x s/c} \cdot R_{Alt} \\ &= \left[T_{inert}^{s/c} \frac{\partial R_{Alt}}{\partial r_{shape}} \begin{pmatrix} \frac{\partial r_{shape}}{\partial x_{inert}} \hat{i} + \\ \frac{\partial r_{shape}}{\partial y_{inert}} \hat{j} + \\ \frac{\partial r_{shape}}{\partial z_{inert}} \hat{k} \end{pmatrix} \right]_{x s/c} \cdot R_{Alt} \end{aligned} \tag{2}$$

In this equation, $T_{inert}^{s/c}$ is a transformation matrix from inertial coordinates to spacecraft-fixed coordinates, Att_x is the attitude offset in the spacecraft-fixed x-direction, and r_{shape} is the radius of the shape model. In Equation 2, the spacecraft-fixed coordinate frame is orientated with the z-direction pointing in the direction that the instruments are pointed. Meanwhile, the xy-plane is aligned with the coordinate frame defined by the line and pixel directions of the optical camera. An equation similar to Equation 2 is written for the partial with respect to the y-direction pointing offset.

To date, when the LIDAR instrument is activated, the altimeter measurements are generally made once per second. This results in an immense amount of data, which increases the run time of the orbit determination software significantly. To overcome this the LIDAR data is decimated to a 10 second minimum time interval between sequential observations. This still provides an adequate density of coverage, while making the processing time more reasonable. Figure 1 shows four different views of the altimeter coverage on Eros, using the decimated LIDAR data collected from April 2 through May 16. In the figure, the black points indicate areas that are covered by LIDAR observations, while the white areas are portions of the surface that have not been covered by the altimeter ground track. As shown, this time span provides substantial coverage of the asteroid. Even after substantially decimating the data, this time span contains over 100,000 observations. It should be pointed out that the altimeter ground track plot does not show the usual smooth orbit pattern associated with most ground track plots due to the variable spacecraft attitude. This is because NEAR, unlike most other altimeter satellites, does not continuously point in the nadir direction. The attitude is constantly changing, in order to point the onboard camera and other instruments in the desired direction. Since the LIDAR instrument is fixed to point in the same direction as the other instruments, the orientation of the altimeter range measurements are continuously changing as well.

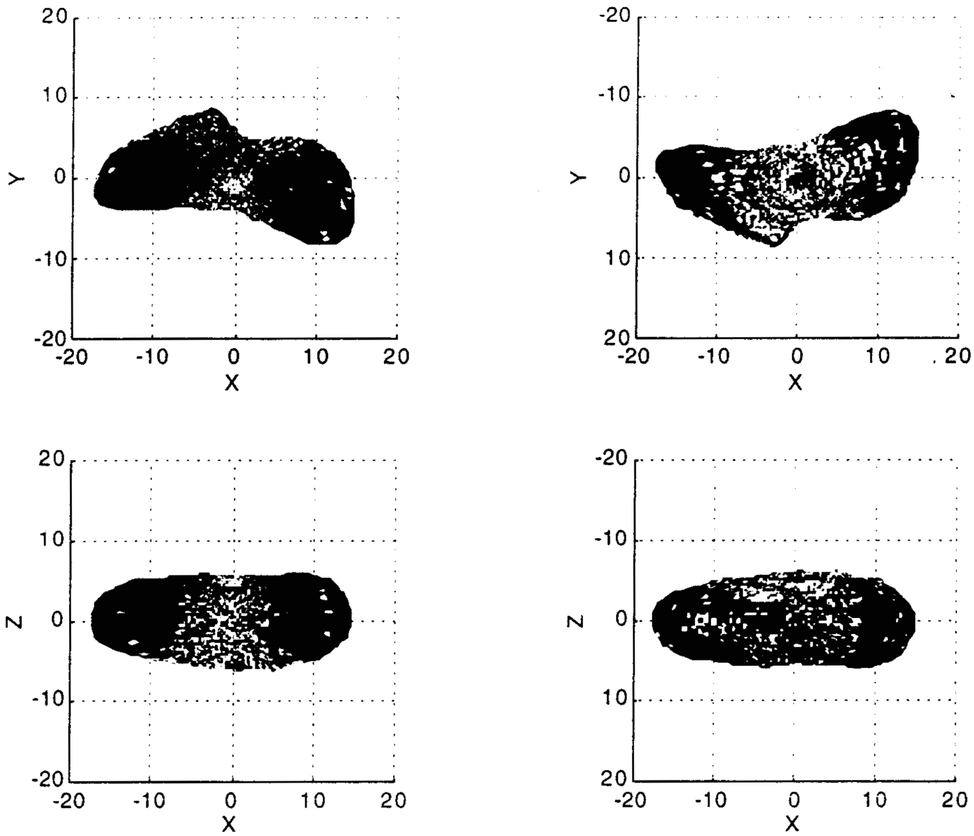

Figure 1 Four views of the LIDAR Ground Track from April 2 through May 16, 2000 (Black areas: LIDAR observations, White areas: No coverage)

Estimating the Shape Model

The Eros shape model is described using spherical harmonic coefficients. To make an estimate of the shape model using the altimeter observations, the operational orbits are used as a reference and are held fixed. This approach insures that there is no aliasing between the shape model coefficients and the orbits. The only parameters that are estimated are the shape model coefficients, through degree and order 20, the LIDAR instrument pointing offsets, the LIDAR range bias, and the LIDAR altitude degradation factor (Eq. 1). All of the parameters are given virtually no a priori constraints, so they are free to adjust. Additionally, LIDAR points are edited from the solution if the residuals are greater than 2 km. The data arc used spans from April 2 through May 16, which is 16 days into the circular 50 km polar orbit phase. It is anticipated that better results will be obtained when more of the 50 km data becomes available and is included in the solution.

Figure 2 View of the Southern Hemisphere of the Eros Shape Model (complete through degree and order 20)

A view of the southern hemisphere of the resulting Eros shape model is shown in Fig. 2. The value of the estimated pointing error is also of interest. The pointing error of the optical camera has been independently determined to be -1.697 mrad in the X-direction, and -0.786 mrad in the Y-direction. In this spacecraft-fixed instrument-pointing coordinate frame, the Z-axis points in the direction that the scientific instruments are designed to point. The estimated values for the LIDAR offset are close to the aforementioned values determined for the camera offset, at -1.93 mrad and 0.46 mrad, respectively. This is important since it seems possible that both the camera and LIDAR instruments could be offset a similar amount, since they are mounted close to each other on the spacecraft. This adds a little more credibility to the values of the estimated offset angles.

The estimate of the range bias is 5.3 m, and the altitude degradation factor is -6.68×10^{-10}. Intuitively, we expect that the degradation factor should be a negative number. This is because as the distance from the asteroid increases, the weakening of the return LIDAR signal would make the measurement longer than the true range since the instrument would not sense the return signal until later. These estimates work out to equate to a LIDAR bias of −865 m at a range of 190 km, which is typical of the spacecraft range early in the orbit arc. When the spacecraft is in the 50 km circular orbit, later in the orbit arc, these estimates result in a LIDAR bias of 3.5 m at a range of 40 km

In order to show the impact of estimating the LIDAR dependent parameters (the pointing offset, bias, and degradation factor), another shape model is estimated without estimating these parameters. The resulting shape model is compared to the shape model obtained previously (in Fig. 2). The two shape models are compared by computing the differences at 2 degree intervals in latitude and longitude. The mean of the differences is 28 m, and the RMS about the mean is 82 m. The differences between the two models is shown graphically in Fig. 3, which shows four different views of Eros. The shading of the figures indicates the amount of difference between the two models.

In Figure 3, few of the differences seem to correspond to orientation changes in the shape models, with the possible exception of some of the differences shown in panel (C). In this panel, the upper left and right faces have large light colored areas, which could correspond to a slight rotation about the X-axis. However, the fact that most of the differences do not seem to correspond to orientation changes is a positive indication that the pointing parameters are being adequately separated from the harmonic coefficients related to the orientation of Eros. This is important since these are the coefficients that might be expected to be the most correlated with the pointing errors. Two aspects are helping provide the separation between the surface harmonics and the pointing errors. First, the orbit altitude and inclination are changing during the orbit arc. This helps by changing the geometry of the LIDAR observations relative to the same surface points, making constant pointing errors distinguishable from errors in the surface model. Similarly, the changing attitude of the spacecraft results in different observation geometry from pass to pass over the same surface points. This non-nadir pointing of the LIDAR instrument is also what provides separation between the range bias and the scale of the shape model.

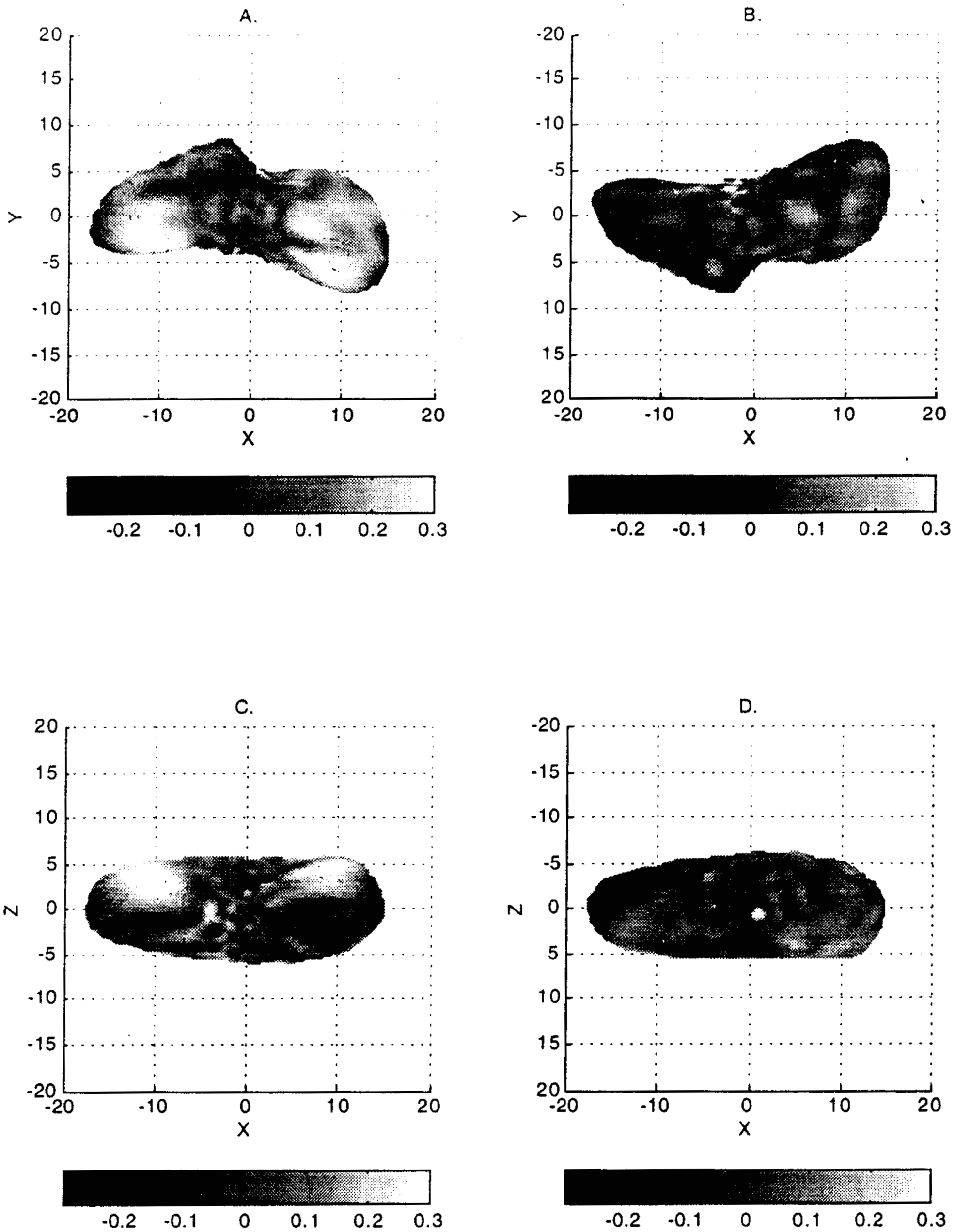

Figure 3 Shape Model Differences (Scale in km)
A. Northern pole view, B. Southern pole view,
C. Negative Y-axis view, D. Positive Y-axis view

In order to show which of these models is more accurate, the solutions for the landmark locations can be used. These landmark locations are obtained from processing the optical navigation data during the reference orbit solution. The radius of the shape models is calculated at the latitude and longitude of each landmark, and compared with the height of the landmark. In this comparison, only the 136 best determined landmarks are used. Currently, these landmarks are all located in the mid-latitudes, corresponding to the areas where most of the spacecraft coverage has been concentrated. Therefore, this comparison does not give a good global evaluation. Nevertheless, it does provide an independent test for the accuracy of the Eros shape models. The results of this comparison are shown in Table 2. It appears that the shape model is more accurate when the LIDAR dependent parameters are accounted for in processing the LIDAR data, as indicated by the reduction in the RMS of the differences from 136 to 109 m.

Since the landmarks are often referenced to craters, the actual reference point can often be located above the surface of Eros. This happens because the reference point is chosen as the center of the ellipse that represents the lip of the crater. The center of this ellipse is then above the floor of the crater. This means that we should expect the mean difference between the height of the landmarks and the shape models, evaluated at the landmark locations, to be positive. This turns out to be the case, as is shown in Table 2.

Table 2

Landmark Solution Heights minus Shape Model Radius

	Estimate LIDAR dependent parameters	Pointing Error not Accounted for
Mean	42 m	85 m
RMS about mean	109 m	136 m

Computing Orbits while Holding the Shape Model Fixed

In this section, the altimeter data is used to help converge the orbits while holding the shape model estimated in the previous section fixed. The accuracy of the orbits computed in this manner will depend on the accuracy of the reference shape model, since errors in the shape model could be aliased into the orbits. To try to quantify the strength of the altimeter observations in orbit determination, the orbits are computed without the optical landmark tracking. These orbits can then be compared to the reference orbits in order to determine the accuracy of the orbits computed with both radiometric and LIDAR data. Although the two sets of orbits are not completely independent since both sets contain the radiometric tracking data, the comparison will still give an indication of the impact that the LIDAR data has on the orbits. The comparison also provides a means to determine the most effective method of processing the LIDAR data.

The orbit arc used for this comparison starts on May 1 and goes through May 10, which means the orbits occur during the circular 50 km polar orbit phase. The same parameters and a priori uncertainties given in Table 1 are used, with the exception of the landmark positions, which cannot be estimated without using the optical data. The radiometric data is also given the same relative weighting as in the reference orbits, while the LIDAR data is given an uncertainty of 400 meters. The LIDAR observations are sampled every 30 seconds, and are edited when the residuals are greater than 600 m.

The LIDAR and DSN orbits are computed in three different ways. In case 1, the orbits are computed without estimating or accounting for any of the LIDAR parameters outlined in Equations 1 or 2. In case 2, the orbits are computed while applying the pointing error that was obtained during the shape model solution, but without including either the range bias or the degradation factor. In case 3, the pointing error, the range bias, and the degradation factor, as determined in the shape model solution are all applied. Additionally the range bias is allowed to adjust minimally, the a priori uncertainty given to the bias is 10 m. The data residuals are summarized for these three cases in Table 3. It is hard to draw any conclusions from the residuals themselves, especially since they are so similar from case to case. It is important that the Doppler residuals do not seem to be adversely affected by the addition of the LIDAR data.

Table 3

RMS of Data Residuals for Orbits Computed with LIDAR data

	DSN Doppler (# of obs / RMS)	LIDAR (# of obs / RMS)
Case 1: No LIDAR parameters estimated	8046 / .00146 Hz	18861 / 93 m
Case 2: Estimate Pointing Error	8046 / .00147 Hz	18876 / 93 m
Case 3: Estimate Point Error, Range Bias, & Degradation Factor	8046 / .00144 Hz	18877 / 92 m

The three cases are now each are compared to the reference orbits. The comparisons are made by differencing each particular test case with the reference orbits every two minutes in the radial, transverse (along-track), and normal (RTN) directions. Plots and statistics of the differences between the reference orbits and the test case orbits are given in Figure 4. From the figure, it is apparent that better agreement with the reference orbits is achieved during each successive test case. For instance, when the pointing error is accounted for (in going from case 1 to case 2), the orbits show a significant improvement in the transverse direction. Likewise, when the range bias and degradation factor are accounted for there is a significant improvement in the radial direction (in going from case 2 to case 3). Improvement in the normal direction is also observed in each successive test case.

However, even in case 3, a 40 m bias remains in the LIDAR orbits. This biasing indicates that there might be an additional error source in the LIDAR data, which is not accounted for properly. Besides an additional pointing error, this could also be due to a time tag error on the LIDAR observation records. Another possible source of error could be changes in performance of the LIDAR instrument as the incident angle with respect to the illuminated surface changes. At the present time, effective methods of determining either of these possible quantities have not been explored.

Computing the Orbits with only LIDAR Data

In this section the orbits are computed without the direct contribution of the radiometric tracking data.. However, these orbits will still have an indirect link to both the radiometric and optical landmark tracking. This indirect contribution is due to the fact that the shape model used was estimated from the reference orbits, which were computed with both the radiometric and optical tracking data.

The same parameters and a priori uncertainties are used as in the last section. The LIDAR dependent parameters are held fixed to the estimates obtained in the long-arc shape model solution. For the 10-day orbit arc, the RMS of the LIDAR residuals is 108 m. Figure 5 shows the RTN differences and statistics between this orbit and the reference orbit. This comparison indicates that the accuracy of the LIDAR-only orbits is somewhere between 100 and 150 m, in a three-dimensional sense.

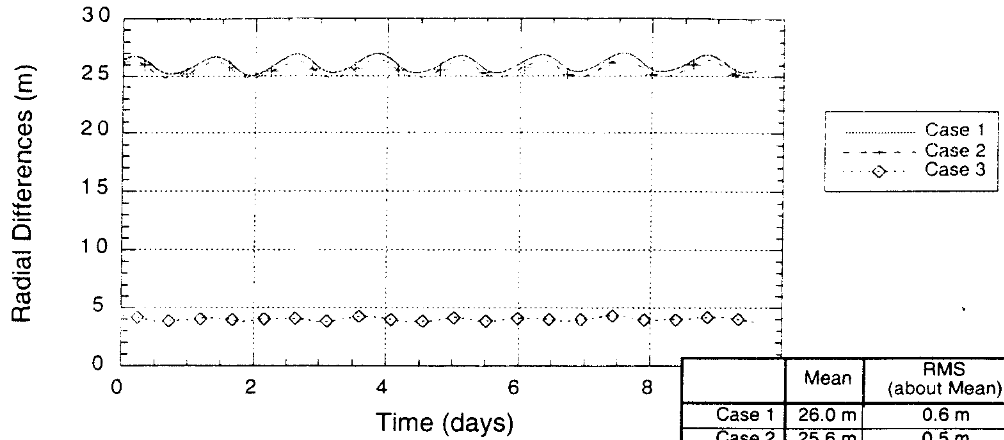

	Mean	RMS (about Mean)
Case 1	26.0 m	0.6 m
Case 2	25.6 m	0.5 m
Case 3	4.0 m	0.1 m

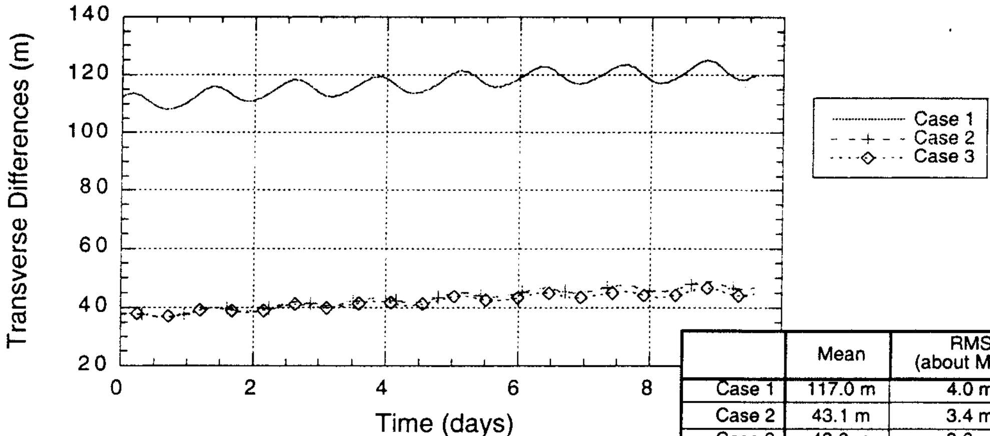

	Mean	RMS (about Mean)
Case 1	117.0 m	4.0 m
Case 2	43.1 m	3.4 m
Case 3	42.0 m	2.6 m

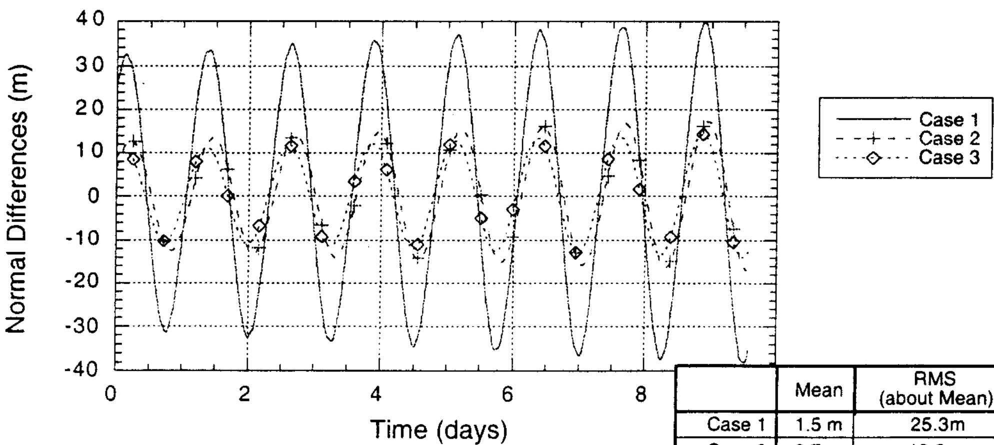

	Mean	RMS (about Mean)
Case 1	1.5 m	25.3m
Case 2	0.7 m	10.6 m
Case 3	0.4 m	8.8 m

Figure 4 RTN Differences between Orbits Computed with LIDAR versus Orbits Computed with Optical Navigation (DSN used in both cases)

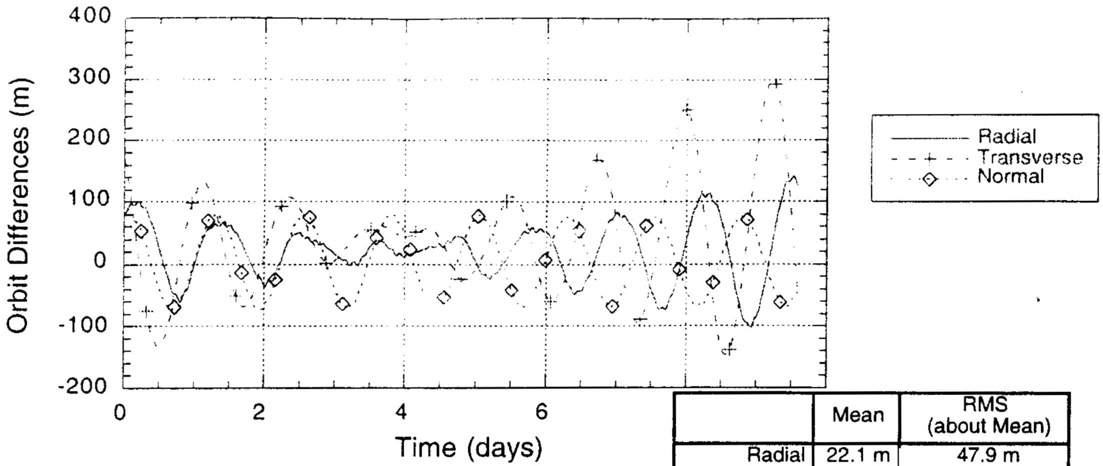

	Mean	RMS (about Mean)
Radial	22.1 m	47.9 m
Transverse	44.3 m	93.0 m
Normal	4.5 m	52.3 m

Figure 5 RTN Differences between Orbits Computed with only LIDAR tracking versus Orbits Computed with DSN and Optical Navigation tracking

Crossover Considerations

In order to improve the impact of LIDAR data on spacecraft navigation, the concept of crossovers can be introduced to assess the accuracy of an orbit and to possibly reach a better estimate.

Crossover points are defined when the altimeter ground track intersects itself on the surface of the orbiting body. The difference in two satellite altimeter ranges interpolated at a crossover point along their respective ground tracks can thus form a new set of data. In theory, these crossover measurements should bear zero-values since the ground track location is the same in both cases. However, errors in the estimate associated with the model will produce residuals that can be minimized to improve some parameters, such as the orbit state.

For NEAR, each LIDAR measurement includes a pointing direction, which is used to determine the illumination point of the observation on the Eros surface (latitude and longitude). Determination of a crossover point will utilize the following technique, as described in Kim.[6]

Let $r_1(t_1)$ and $r_2(t_2)$ be two ground track trajectory vectors referenced to the Eros body fixed frame, where t_1 and t_2 are time-tags used as independent variables of the two trajectories. The ground track crossing condition for the two trajectories can be simply written as:

$$\hat{r}_1(t_1) = \hat{r}_2(t_2) \tag{3}$$

where $\hat{r}_1$ and $\hat{r}_2$ are Eros-centered unit vectors pointing in the direction of r_1 and r_2, respectively. Let F denote the direction cosine between $\hat{r}_1$ and $\hat{r}_2$, i.e.:

$$F(t_1,t_2) = \hat{r}_1(t_1)\cdot\hat{r}_2(t_2) \tag{4}$$

Locating ground track crossovers can be considered a two-dimensional root-finding problem of a single scalar equation

$$F(t_1,t_2) = 1 \tag{5}$$

which replaces the vector condition in Equation 3. Since F yields its maximum value of 1 at a crossover, the problem can be solved by using the following condition.

$$\begin{aligned} \frac{\partial F}{\partial t_1} &= \dot{\hat{r}}_1\cdot\hat{r}_2 = 0 \\ \frac{\partial F}{\partial t_2} &= \hat{r}_1\cdot\dot{\hat{r}}_2 = 0 \end{aligned} \tag{6}$$

Given a point $\{t_1, t_2\}$ close to a crossover solution, the Newton-Raphson iteration scheme

$$\begin{Bmatrix} t_1 \\ t_2 \end{Bmatrix} \leftarrow \begin{Bmatrix} t_1 \\ t_2 \end{Bmatrix} - \begin{bmatrix} \ddot{\hat{r}}_1\cdot\hat{r}_2 & \dot{\hat{r}}_1\cdot\dot{\hat{r}}_2 \\ \dot{\hat{r}}_1\cdot\dot{\hat{r}}_2 & \hat{r}_1\cdot\ddot{\hat{r}}_2 \end{bmatrix}^{-1} \begin{Bmatrix} \dot{\hat{r}}_1\cdot\hat{r}_2 \\ \hat{r}_1\cdot\dot{\hat{r}}_2 \end{Bmatrix} \tag{7}$$

may converge to a solution. Furthermore, a converged solution will yield a crossover when Equation 3 is satisfied.

The associated crossover measurement is the difference between the respective ground track trajectory vectors r_1 and r_2, interpolated at t_1 and t_2 respectively. Information on the magnitude of r_1 and r_2 can be obtained using either the shape model or a combination of the spacecraft trajectory and LIDAR measurement. This technique is currently under testing and results have yet to be determined.

Summary

This study has attempted to quantify the impact of adding altimeter range observations into the orbit determination problem when a spacecraft is orbiting a small body. The analysis was done using LIDAR data from the NEAR spacecraft, which is currently orbiting the asteroid Eros. By holding the orbits computed with radiometric and optical data fixed, the altimeter range data is successfully used to estimate an Eros shape model. Also, during this process estimates for the LIDAR pointing error, range bias, and altitude degradation factor were obtained. The value for this pointing error is close to the independently observed pointing error for the camera, making the estimate more credible. The shape model also agrees at the 100 m level with the landmark heights, which are determined through the optical tracking data.

The orbits computed with the LIDAR data and the radiometric data together agree with the operational orbits at about the 40 to 50 m level. Even after estimating a pointing error, range bias, and degradation factor, the LIDAR data seems to bias the orbits, especially in the transverse direction. The complete cause and fix for this biasing have yet to be determined. Likely causes of this could be time tag errors, instrument performance problems, or additional pointing errors that are not accounted for.

Estimating the orbits using just the LIDAR data was evaluated. This resulted in a degradation of the accuracy of the orbits to the 100 to 150 m level. For future missions, this level of accuracy may be acceptable, however these results were obtained by using the radiometric and optical data to help create the reference shape model.

As the mission progresses, more and more LIDAR data will be accumulated. This data, especially in the 50 km and 35 km orbits, will allow the processing techniques to be further refined. Hopefully, this will also shed some light on the cause of the biasing ot the orbits estimated with the LIDAR data. Also, adding an algorithm to process altimeter crossovers in the orbit determination software may prove beneficial. This type of measurement would eliminate errors in the shape model from being aliased into the estimated orbits. This may give more strength to the altimeter data, and make it a more valuable tool, in terms of orbit determination.

Acknowledgement

The work described in this paper was funded by the TMOD Technology Program and performed by the Jet Propulsion Laboratory, California Institute of Technology under a contract with the National Aeronautics and Space Administration.

References

[1] Farquhar, R.W., "Introduction: The Near-Earth Asteroid Rendezvous (NEAR) Mission," *The Journal of the Astronautical Sciences*, Vol. 43, No. 4, pp 349-352, October-December 1995.

[2] Farquhar, R.W., Dunham, D.W., and McAdams, J.V., "NEAR Mission Overview and Trajectory Design," *The Journal of the Astronautical Sciences*, Vol. 43, No. 4, pp 353-372, October-December 1995.

[3] Miller, J.K., P.G. Antreasian, R.W. Gaskell, J. Giorgini, C.E. Helfrich, W.M. Owen, B.G. Williams, and D.K. Yeomans, "Determination of Eros Physical Parameters for Near Earth Asteroid Rendezvous Orbit Phase Navigation," *AAS/AIAA Astrodynamics Specialist Conference*, Girdwood, AK, August 16-18, 1999, Paper AAS99-463.

[4] Helfrich, C.E., J.K. Miller, P.G. Antreasian, E. Carranza, B.G. Williams, D.W. Dunham, R.W. Farquhar, J.V. McAdams, "Near Earth Asteroid Rendezvous (NEAR), Revised Eros Phase Trajectory Design," *AAS/AIAA Astrodynamics Specialist Conference*, Girdwood, AK, August 16-18, 1999, Paper AAS99-464.

[5] Bordi, J.J., P.G. Antreasian, J.K. Miller, and B.G. Williams, "Altimeter Range Processing Analysis for Spacecraft Navigation about Small Bodies," *AAS/AIAA Space Flight Mechanics Meeting*, Clearwater, Florida, January 23-26, 2000, Paper AAS00-165.

[6] Kim, M.C., "Theory of satellite ground track crossovers", *Journal of Geodesy*, Vol. 71, pp 749-767, 1997.